BULLETIN OF THE POLISH ACADEMY OF SCIENCES
TECHNICAL SCIENCES, Vol. 70(1), 2022, Article number: e140257
DOI: 10.24425/bpasts.2022.140257

Power quality management in electrical rid using SCANN controller-based UPQC

Balaji VARADHARAJAN[1]*, and Chitra SUBRAMANIAN[2]

[1] Department of Electrical and Electronics Engineering, Kumaraguru College of Technology, Coimbatore, Tamilnadu – 641049, India and Research Scholar (Electrical), Anna University, Chennai, Tamilnadu, India

[2] Department of Electrical and Electronics Engineering, Government College of Technology, Coimbatore, Tamilnadu – 641049, India

Abstract. The electrical grid integration takes great attention because of the increasing population in the nonlinear load connected to the power distribution system. This manuscript deals with the power quality issues and mitigations associated with the electrical grid. The proposed single comprehensive artificial neural network (SCANN) controller with unified power quality conditioner (UPQC) is modelled in MATLAB Simulink environment. It provides series and shunt compensation that helps mitigate voltage and current distortion at the end of the distribution system. Initially, four proportional integral (PI) controllers are used to control the UPQC. Later the trained SCANN controller replaces four PI Controllers for better control action. PI and SCANN controllers' simulation results are compared to find the optimal solutions. A prototype model of SCANN controller is constructed and tested. The test results show that the SCANN based UPQC maintains grid voltage and current magnitude within permissible limits under fluctuating conditions.

Key words: SCANN; UPQC; total harmonic distortion; particle swarm optimization.

1. INTRODUCTION

The development of industrial and domestic solid-state high-power electronics devices technology is progressing rapidly. The power electronic components may produce higher order harmonics, and its total harmonic distortion (THD) value affects the power quality in various aspects of the entire electrical system. E. Hossain *et al.* [1] presented a paper on comparing the various performance indices with different topologies and control schemes of the compensation system. To analyze the stable operation, it is tested with different types of compensation devices such as STATCOM, DVR, SSSC and UPQC for microgrid systems. The comparison results show that the UPQC can be a potential choice for real power management due to its several advantages. In contrast, the spinning reserve can enhance the power quality in the electrical grid. J. Ye *et al.* [2] investigated an important issue associated with the shunt and series conversion system addressed with inverters data-driven control-based controller. It is proposed with different phase angle control methods to analyze the unified power quality conditioner (UPQC) system implementation at a minimal cost. S. Chandrakala Devi *et al.* [3] presented a modified second-order generalized integrator for estimating load current of grid implemented with Solar PV integrated UPQC to provide clean energy has been presented. S. Silva *et al.* [4] provide a complete evaluation and comparative analysis for finding static and dynamic performances of a three-phase UPQC. It was developed with a controller to operate using conventional and dual/inverted compensation strategies for active power-line conditioning. S.B. Karanki *et al.* [5] presented a paper on particle swarm optimization (PSO) analyzed with UPQC integrated with real power photovoltaic and storage battery system. From the side of control strategy, a PI-based modified control scheme has been implemented for UPQC to compensate the voltage sag, swell, and total harmonic distortion (THD) in the distribution system subsequently to improve the power quality [6–8]. The next level of the literature review is based on the UPQC based multi-level inverter (five-level MLI) with DC link conversion enabled with ANN controller helps improve the voltage and current profile. The performance of the active filter is experimented with nonlinear loads and harmonic distortion voltage [9, 10]. The active filter injects active and reactive power supply with the aid of DC conversion system. It is operated with a proposed hybrid backpropagation controller [11–14]. C.K. Sundarabalan *et al.* [15] proposed a system that real power is injected through a fuel cell (FCI-UOQC) in the place of capacitor DC link. Also, it has been proposed with modified four-leg inverter on shunt current control and three leg inverters on series voltage controller. The control algorithm implements proportional-integral with offline data trained ANFIS controller. M. Ochoa-Gimenez *et al.* [16] experimented with a comprehensive control strategy for UPQC to address power quality problems. A dedicated three controllers are designed. The first controller is responsible for active and reactive power flow. The second is a harmonic controller that takes care of zero-error tracking for voltage and current harmonics compensation. Last and the third controller does the operation of the set-point generation block. In addition, a pulse width modulation (PWM)-based modulation with fixed switching frequency is used for both converters.

*e-mail: cnt2gee@gmail.com

Manuscript submitted 2021-07-09, revised 2021-11-01, initially accepted for publication 2021-12-10, published in February 2022.

U.K. Renduchintala and C. Pang [17] demonstrate the power quality improvement of grid-interactive microgrids. The proposed system presents power control strategies using a single-stage converter to compensate for the microgrid system. This microgrid is integrated with a single converter and applied to maximum renewable power utilization with minimal losses. In addition, it is proposed that the neuro-fuzzy controller helps for frequency tracking and removal of harmonics in grid voltage and load currents. P. Falkowski *et al.* [18] presented a paper on UPQC with an extended search algorithm to enhance the power quality. The control signals required are produced by comparing the reference and actual signals of the bus and DC link voltage. A phase-locked loop (PLL) is also used to provide the power factor compensation. Bijan Rahmani, Weixing Li and Guihua Liu investigated an improved synchronous reference frame (SRF) well-appointed with a wavelet-based PLL to regulate the shunt active power filter. The fundamental source voltage at the positive sequence is used as the input signal to PLL. The control signals generated by the SRF-based compensation algorithm match the SAPF's reference with the power grid. An improved series filter (SF) is used for the current harmonic suppression loop. Parallel operation of the SAPF and SF is organized with UPQC. A photovoltaic (PV) system is used instead of DC-link capacitor in UPQC [19, 20].

Most of the literature deals with the different control algorithms, likely SRF, fuzzy and neuro-fuzzy etc., with a larger number of controllers for controlling UPQC to improve the power quality. It is needed that an UPQC with an optimal control algorithm and the intelligent controller is required to maintain the power quality and withstand power system fluctuations to provide real power support for the distribution system. Mathematical modelling with a comprehensive control scheme is required.

This paper adopts a novel single comprehensive artificial neural network (SCANN) controller with UPQC. The Mathematical modelling of SCANN controlled UPQC is simulated in MATLAB Simulink environment, and the test results are evaluated.

2. PROPOSED METHODOLOGY

The Mathematical modelling of SCANN controller is adopted for simulation technique in place of four conventional proportional integrated differential controllers. The work management ensures the optimal effectiveness of the system to provide real power support to the distribution system. A simulation is developed to model UPQC compensation system under MATLAB environment. The compensation system consists of four PI operation controllers. Out of four controllers, two controllers work for shunt compensation, and the next two controllers serve for series compensation to provide the real and reactive power control. The four PI control parameters have been collected and used for training ANN controller as shown in Fig. 1. After that, a single comprehensive ANN is developed instead of four PI controllers, which merges all four single ANN operations.

3. MODELLING OF CONTROL TECHNIQUE

3.1. The DQ transformation

The grid supply voltage (V_{abc}) is supposed to be sinusoidal in nature. The control system for power management requires the steady-state equivalent of DC quantities from AC source requires conversion called DQ transformation technique. This system converts equivalent real and reactive (V_{dq0}) power axis operational quantities such as the load voltage divided into two quantities. The first one is the active component, and the other is injected parameters such as negative sequence voltage, har-

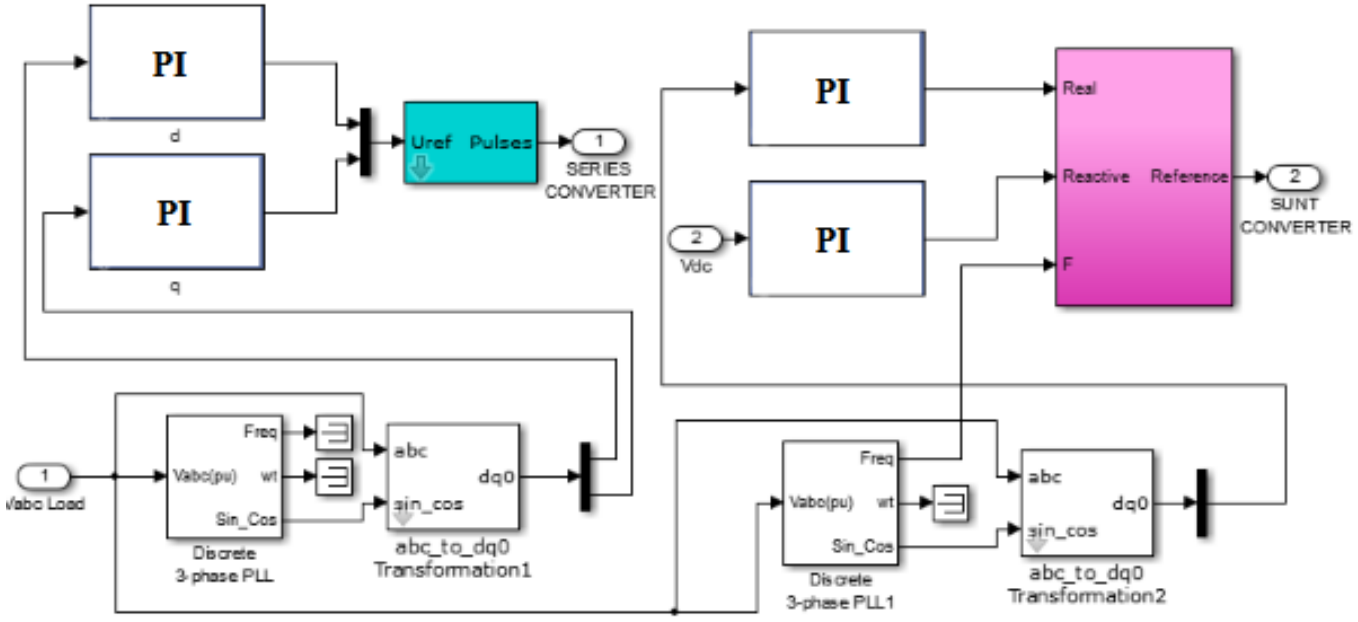

Fig. 1. Four-model PI controller

monic voltage, and reactive voltage. These are the appropriate quantity needed to compensate for the system parameters. Hence, the active series filter serves the purpose of voltage control. The active shunt filter is responsible for current control, so the two parts separate the load voltage as in equation (1).

$$V_L = V_{LP} + V_C\,, \tag{1}$$

where, V_L – load voltage, V_{LP} – active component, V_C – compensation voltage. A 120° phase shift of three-phase voltage is required to achieve the control. A $dq0$ transformation can be aided to attain it by using a synchronous $dq0$ reference frame with the function of sine and cosine Park's transformation. The UPQC simulation system uses a phase-locked loop block to convert the AC quantity V_{abc} to equal DC quantity V_{dq0}. It consists of d, q and 0 axis parameters used to position the rotating frame. It can be given by ωt, where ω reference to the speed of the d-q frame. The reference voltage can be obtained by framing the equation (2) and equation (3).

$$\begin{bmatrix} V_d \\ V_q \\ V_O \end{bmatrix} = \begin{bmatrix} \sin\theta & \sin\theta{-}120^\circ & \sin\theta{+}120^\circ \\ \cos\theta & \cos\theta{-}120^\circ & \cos\theta{+}120^\circ \\ \frac{1}{2} & \frac{1}{2} & \frac{1}{2} \end{bmatrix} \begin{bmatrix} V_a \\ V_b \\ V_c \end{bmatrix}, \tag{2}$$

$$\begin{bmatrix} V_d \\ V_q \\ V_O \end{bmatrix} = \begin{bmatrix} \sin\theta & \cos\theta & 1 \\ \sin\theta{-}120^\circ & \cos\theta{-}120^\circ & 1 \\ \sin\theta{+}120^\circ & \cos\theta{+}120^\circ & 1 \end{bmatrix} \begin{bmatrix} V_a \\ V_b \\ V_c \end{bmatrix}. \tag{3}$$

The sinusoidal grid phase voltages (V_{abc}) are time-varying vector quantities displaced by 120° phase shifts from one another. If the connected loads are resistive in nature, the source side power factor is unity and load voltage, and the load current profile is set as optimal. Unfortunately, the connected loads are nonlinear, like electronically operated devices. Both the source and load sides may have unbalanced operating parameters. The intelligence algorithm is set to provide fast response, and the ability to provide robust compensation, power quality and better control during abnormal operating times becomes essential.

3.2. Classification of the controller

As the first step, a set of four PI controllers were designed. One set of controllers is used to control the shunt converter, and another set is used for the series converter. These four PI controllers are regulated suitably to deliver the expected performance. After attaining appropriate performance, the controller input and output data are collected from four PI controllers. The four input and output data are trained with the neural network fitting tool and generate a single ANN block by MATLAB software.

3.3. Design of PI controller

The UPQC system is connected with a nonlinear load so that fixed PI control parameters may produce inaccurate and undesirable response under dynamic operating conditions. The desired response is achieved by tuning the PI controller using the Ziegler–Nichols method with MATLAB "*sisotool*". The equation form of PI controller is given by the PI functional equation (4) can be described by:

$$u(t) = K_p e(t) + K_i \int_0^t e(t)\,\mathrm{d}t, \tag{4}$$

where, $u(t)$ – output response of the PI controller, K_p and K_i the proportional gain and integral gain, respectively, e is the error value is taken as an input of the PI controller shown in Fig. 2. The DC power required to maintain real power can be expressed as equation (5).

$$P_{dc} = K_p\,(V_{\mathrm{ref}} - V_{\mathrm{act}}) + K_i \int_0^t (V_{\mathrm{ref}} - V_{\mathrm{act}})\,\mathrm{d}t. \tag{5}$$

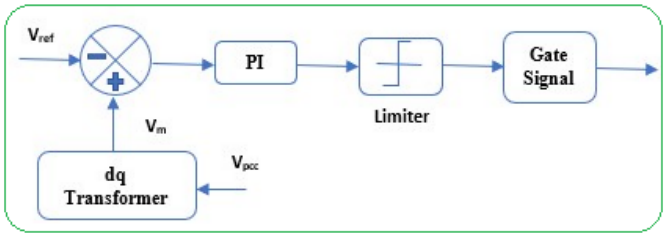

Fig. 2. PI control block diagram

The measured voltage $V(t)_{\mathrm{act}}$ and reference voltage $v(t)_{\mathrm{ref}}$, the d axis and q axis parameters are taken in per unit values (unit value of 1). The error $u(t)$ will be equal to zero when the K_p and K_i value becomes one. The obtained V_{act} is compared with V_{ref}. Based on that, the K_p and K_i value can be dynamically adjusted to match the measured and reference voltage. The DC link voltage of the UPQC system is measured at regular intervals and compared with the reference and V_{act} that helps for the transformation of real power with V_{dc}.

The design of four model PI controllers is shown in Fig. 2. The controller design consists of four operational parameters. Out of this, the first two controllers get output voltage from measurement sensors and convert it into d-q transformation, which can be used to inject voltage into the source side of the grid using a series active filter and another two control input parameters of V_{dc} and V_{abc} are used to supply reactive current by shunt active filter.

3.4. DC link voltage

The main function of the DC capacitor voltage (V_{dc}) controller is to inject voltage using shunt active filter. The real power shall be transferred to exchange the charging current from AC system to DC link capacitor can be given by equation (6).

$$V_{dc} = \frac{1}{C_{dc}} \int i_{dc}\,\mathrm{d}t, \tag{6}$$

The reactive power (Q_{inv}) is controlled by the quadrature axis current of shunt active filter I_{sh}, where the reference can be

found from PI controller tuned parameter. Reactive power can be maintained constant by reference reactive power (Q_{in} and V_{ref}) equation (7).

$$i(k)_{\text{shq\_ref}} = i(k-1)_{\text{shqref}} + K_P\left[Q(k)_{\text{inv\_error}} - Q(k-1)_{\text{inv\_error}}\right] + K_I\left[Q(k)_{\text{inv\_error}}\right]. \tag{7}$$

The shunt active filter controls the current source thereby compensates the harmonic, reactive and negative sequence components in load current as given in equation (8)

$$i_l = i_s + i_{\text{sh}}. \tag{8}$$

The system voltage and current values are observed at the appropriate point (PCC) of the transmission line, and it must be converted into d-q component by Park's transformation. The desired reference parameter can be attained by comparing the operating parameter with the error signal and processing it in the PI controller.

3.5. Artificial neural networks

Artificial neural network (ANN) is a powerful soft computing technique tool used for perfect pattern matching between input and output with faster system response. The Levenberg trains the collected UPQC parameters – Marquardt back propagation (LMBP) technique, and the error can be minimized by the mean square error method (MSE). The conventional controller does not meet desired response for comprehensive and dynamic variation of a system parameter. The LMBP method will give faster convergence and dynamic response power transaction appropriate duration in the distributed parameter of active filters the functional equation as follows.

$$C = [V_e(K)], \tag{9}$$

$$V_e = V_{dc}^* - V(k)_{dc}. \tag{10}$$

Functional error is represented as

$$Z(K) = V(k)_{\text{out}} - V(k-1)_{\text{out}}. \tag{11}$$

The control signal is produced by neuron cell, and it can be stated as

$$c(K) = c(K-1) + \sum_{i=1}^{2} w_i(k)x_i(K). \tag{12}$$

Sampling time of weight of neuron cell at $(k+1)$ can be described as

$$W_i(k+1) = (1-r)W_i(k) + \eta Z(k)c(k)x_i(k), \tag{13}$$

where η – learning rate, r – constant for convergence, $W_i(k)$ at k-th step is arrived by equation (13). $W_i(k)$ can be mentioned as

$$\Delta W_i(k) = W_i(k+1) - W_i(k) - r\left[W_i(k) - \frac{\eta Z(k)x_i(k)u(k)}{r}\right]. \tag{14}$$

Function of post and pre value of synaptic signals can be calculated using F_i.

$$\Delta W_i(k) = F_i\left(I_{isp}(k), x_i(k)\right), \tag{15}$$

$$\frac{\partial F_i}{\partial W_i} = \frac{W_i(k) - \eta Z(k)x_i(k)u(k)}{r}. \tag{16}$$

Change of weight in k-th step is noted as

$$\partial W_i(k) = -r\frac{\partial F_i(k)}{\partial W_i(k)}. \tag{17}$$

The trained 5000 data are collected from the modelled four PI controllers simulated under sag, fault, swell, and dynamical change in load condition specified duration. The collected data of active and reactive power, common coupling voltage and load voltage are used to train the ANN fitting tool. The trained parameters were 70%, 15%, and 10% training validated and tested.

ANN functional flow chart is shown in Fig. 3. During the training, ANN provides appropriate functioning of the hidden layer. It is activated parallels, and if the error is found in the trained parameter data, the backpropagation process can rectify it. Then it will be iterated a number of times, and the trained parameters are compared with the target value. The iteration will go on until the target value finds close with the convergence value so that the optimal operating point is said to be achieved.

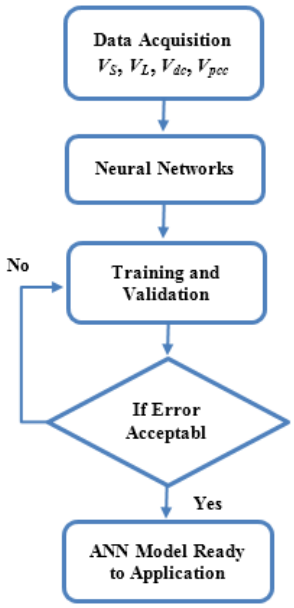

Fig. 3. ANN functional flowchart

3.6. SCANN controller

The proposed SCANN controller model is constructed from the conventional four PI controller model, as shown in Fig. 4. The UPQC series and shunt active filter control parameters are collected under different configurations such as sag, swell, fault, and dynamic load change conditions. The conventional controller of series and shunt active system requires four individ-

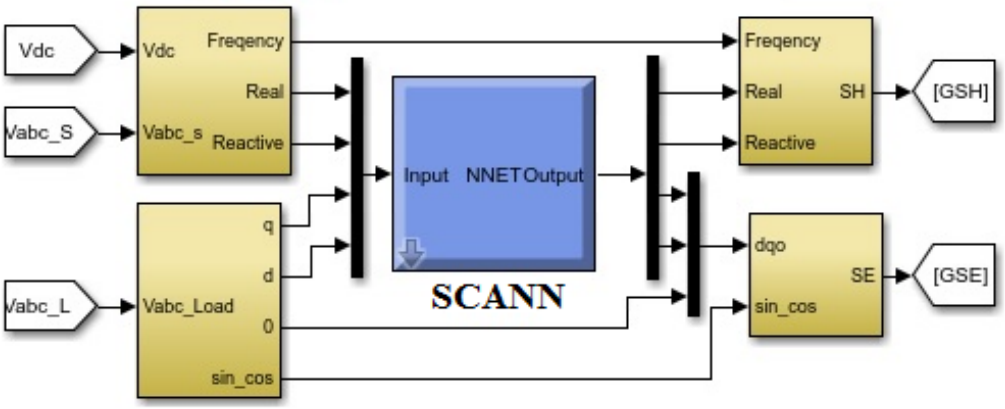

Fig. 4. SCANN controller

ual PI controllers. The controller parameters are selected based on Ziegler–Nichols method to attain optimal stable operational value.

After eliminating the four PI, it is adopted with a single comprehensive ANN controller to control the UPQC. It is simulated and analyzed for different operating circumstances. The simulation is configured with the proposed controller under different loading conditions. It will help mitigate the power quality issues, thereby improving the performance of the overall UPQC system.

4. SIMULATION RESULTS AND DISCUSSIONS

To evaluate the performance of the proposed SCANN controlled UPQC system, it is simulated in MATLAB/Simulink environment as shown in Fig. 5. The system consists of six pulse shunt and series active filters with a DC link voltage conversion system is tested with both conventional and proposed intelligence algorithms as shown in Table 1.

Table 1
System parameter

Description	Rated Value
Source voltage	23 kV
Operating frequency	60 Hz
Load details (R/L/C)	10 kΩ/100 μH/100 μF
DC link capacitor	10000 μF
Shunt converter transformer	25 kV/10 kV, 100 kVA
Series converter transformer	25 kV/10 kV, 100 kVA
Filter (inductance/capacitor)	10 mH/10 mF

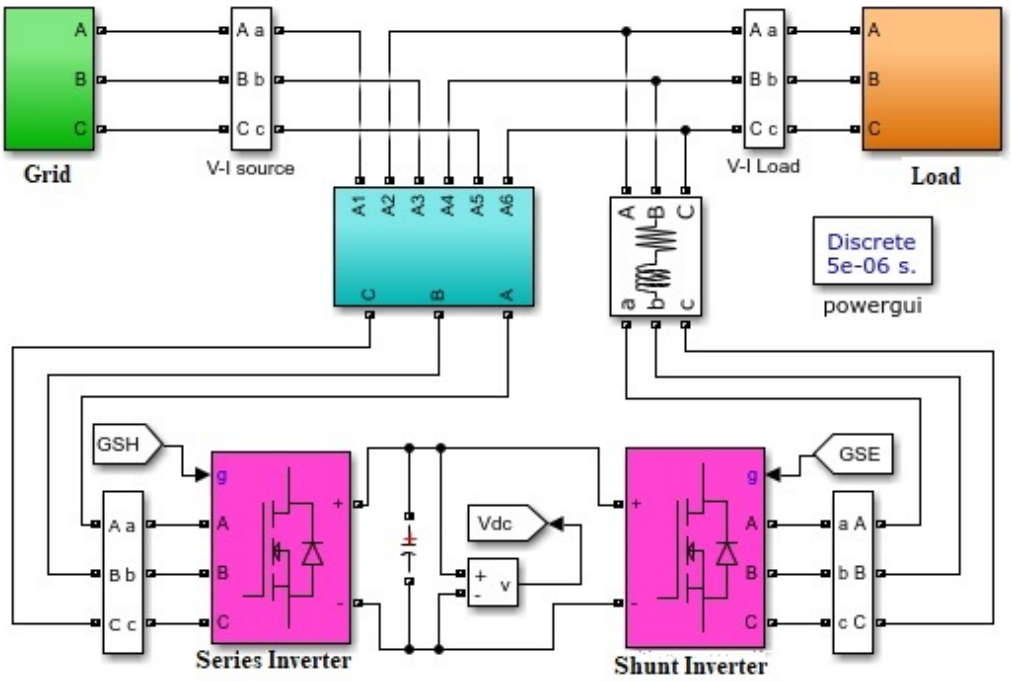

Fig. 5. UPQC simulation model

4.1. Simulation study

A Comparative study is done for both controllers to find the performance of converters under sag and swell conditions. Also, the transient response of converters is analyzed during fault conditions. Furtherly, the performance of converters is monitored during dynamic load conditions. Moreover, the THD levels are recorded at the load side to optimize the controller parameters.

Figure 6 to Fig. 9 shows the different operating parameters under different working conditions obtained during simulation. The performance of the UPQC using SCANN based controller can be esteemed by matching the results of the new scheme with the popular multiple PI controllers-based schemes. The system simulation is carried out, and the results of various configurations are illustrated in Fig. 6 to Fig. 9.

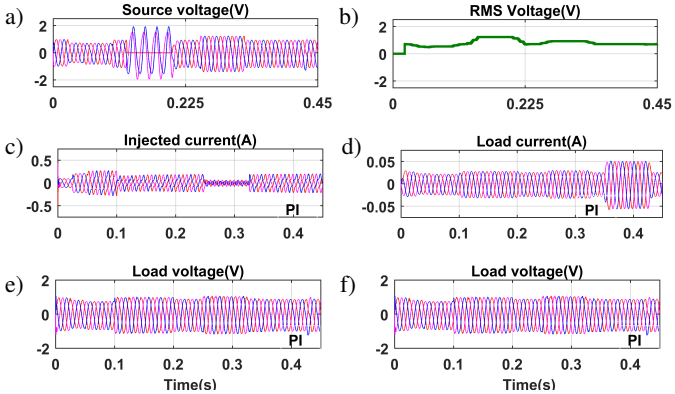

Fig. 6. Simulation result of PI controller (a) source voltage (b) RMS source voltage (c) DC link injected current (d) load current (e) injected voltage (f) load voltage

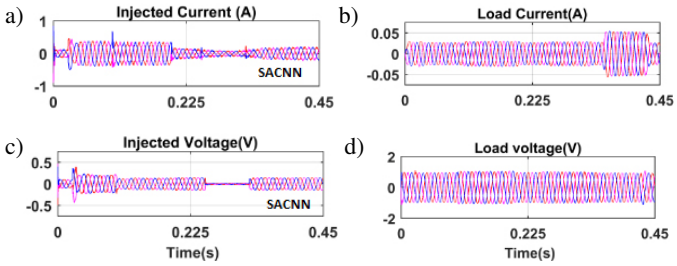

Fig. 7. Simulation result of SCANN algorithm: (a) injected voltage, (b) load voltage, (c) injected current, (d) load current

4.2. Simulation study

A Comparative study is done for both controllers to find the performance of converters under sag and swell conditions. Also, the transient response of converters is analyzed during fault conditions. Furtherly, the performance of converters is monitored during dynamic load conditions. Moreover, the THD levels are recorded at the load side to optimize the controller parameters. Figure 6 to Fig. 9 show the different operating parameters under different working conditions obtained during simulation. The performance of the UPQC using SCANN based controller can be esteemed by matching the results of the new scheme with the popular multiple PI controllers-based schemes. The system simulation is carried out and results of various configurations are illustrated in Fig. 6 to Fig. 9.

The traditional PI and proposed SCANN control techniques are compared, and the detailed performance results are given in Table 2. The simulation results show that the SCANN controller shows significant results in terms of THD and magnitude when compared with PI controller outputs.

Table 2
Simulated results of PI and SCANN controller

Parameters	PI			SCANN		
Load voltage (p.u.)	Magnitude	RMS	THD%	Magnitude	RMS	THD%
Sag	0.74	0.58	13.40	0.95	0.67	4.23
Fault	0.95	0.74	10.45	1.02	0.755	3.15
Swell	1.03	0.77	9.48	1.01	0.71	2.86
Dynamic load	0.86	0.66	12.64	0.92	0.66	2.05
Load current (p.u.)	Magnitude	RMS	THD%	Magnitude	RMS	THD%
Sag	0.023	0.016	8.47	0.026	0.019	3.32
Fault	0.026	0.021	6.12	0.028	0.021	2.12
Swell	0.029	0.022	6.51	0.029	0.020	1.68
Dynamic load	0.050	0.037	8.39	0.052	0.038	4.67

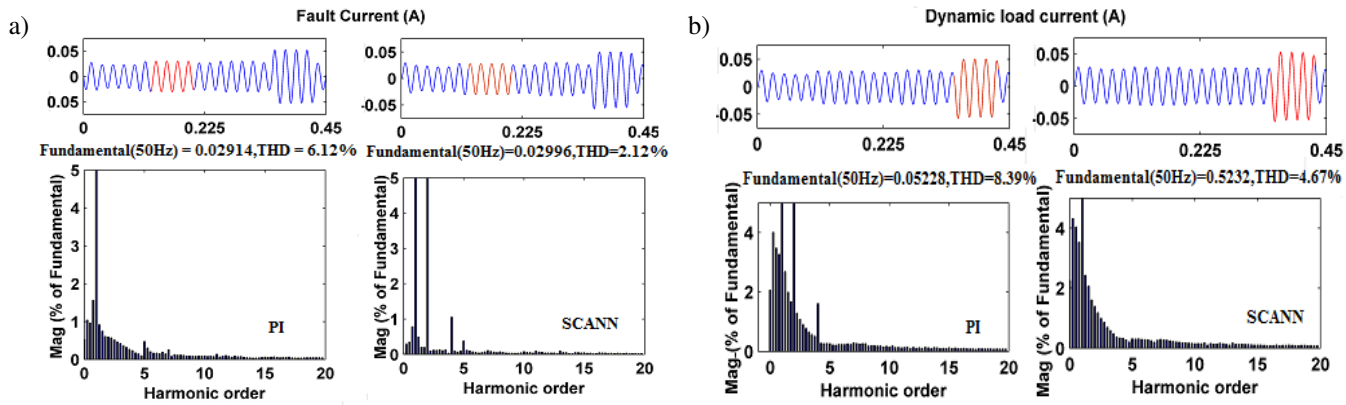

Fig. 8. Simulated result of THD analysis of PI and SCANN Load current

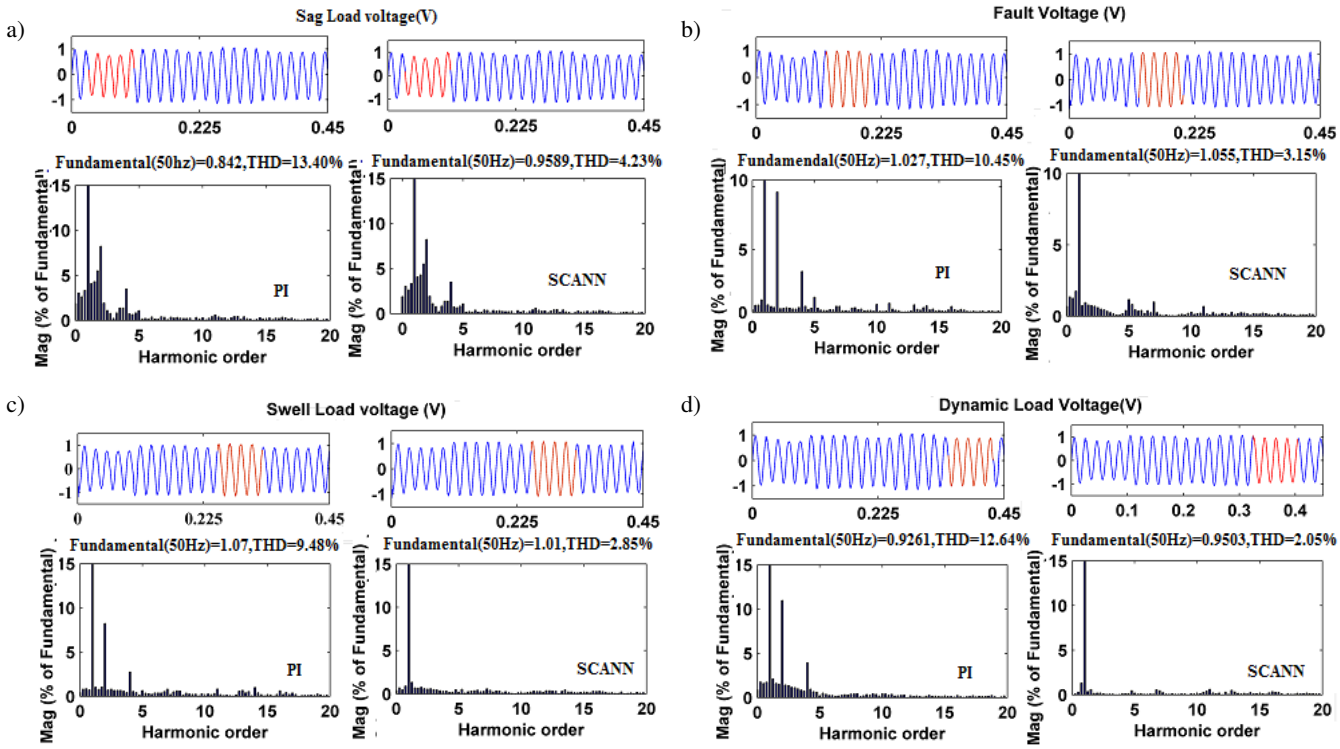

Fig. 9. Simulated result of THD analysis of PI and SCANN controller

5. EXPERIMENTAL PROTOTYPE MODEL

The experimental setup is constructed to test and validate the proposed idea. A prototype model is developed with two numbers of ATMEL 89c51 micro controllers. One of the micro controllers monitors the power factor and displays it in an LCD unit. The other micro controller is used to transmit and receive the data to and from a PC. The data required for processing are the source voltage (V_{abc}), the load side three-phase voltage (V_{LP}) and the DC link voltage. These voltages are logged into the PC through the serial interface facility of the second 89c51 micro controller. A third micro controller, the PIC 16F877A, collects the analogue signals and converts them into digital data to perform the required *d-q* transformations. The collected data are fed to the micro controller 89c51 to buff the personal computer (PC).

The PC is the actual controller. The information regarding the source, load voltages and the DC link voltage are translated into V_{ds}, V_{qs}, V_{dl}, V_{ql} and V_{dc}, which are supposed to be used in the PI embedded C program. The control strategy's block schematic is quite similar to that used in the MATLAB/SIMULINK simulation, as shown in Fig. 5. A comparative study is made on three-phase induction motor as load. Initially, the motor is connected to three-phase sources without ANN compensation. The motor is tested for sag and swell conditions. Later the motor is supplied through ANN controller and tested for sag and swell conditions. Both the source side and load side voltages and currents values are recorded. The DC link capacitor voltage is also captured for each case.

The experimental setup is validated based on the simulation performance of SCANN algorithm, as shown in Fig. 10. The experimental results in terms of THD voltage and current levels after compensation are shown in Table 3. Due to the action of shunt converter, the load currents are balanced and become sinusoidal. Hence the ANN controller helps for harmonic elimination and voltage compensation.

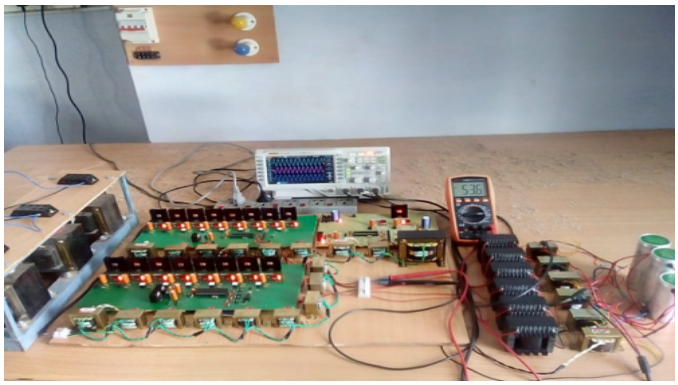

Fig. 10. The hardware setup of SCANN based UPQC

Table 3
Experimental result of hardware prototype

Description	Source THD%	Load THD%
Sag voltage	5.01	4.23
Sag current	4.12	3.35
Swell voltage	3.51	2.52
Swell current	2.52	1.95

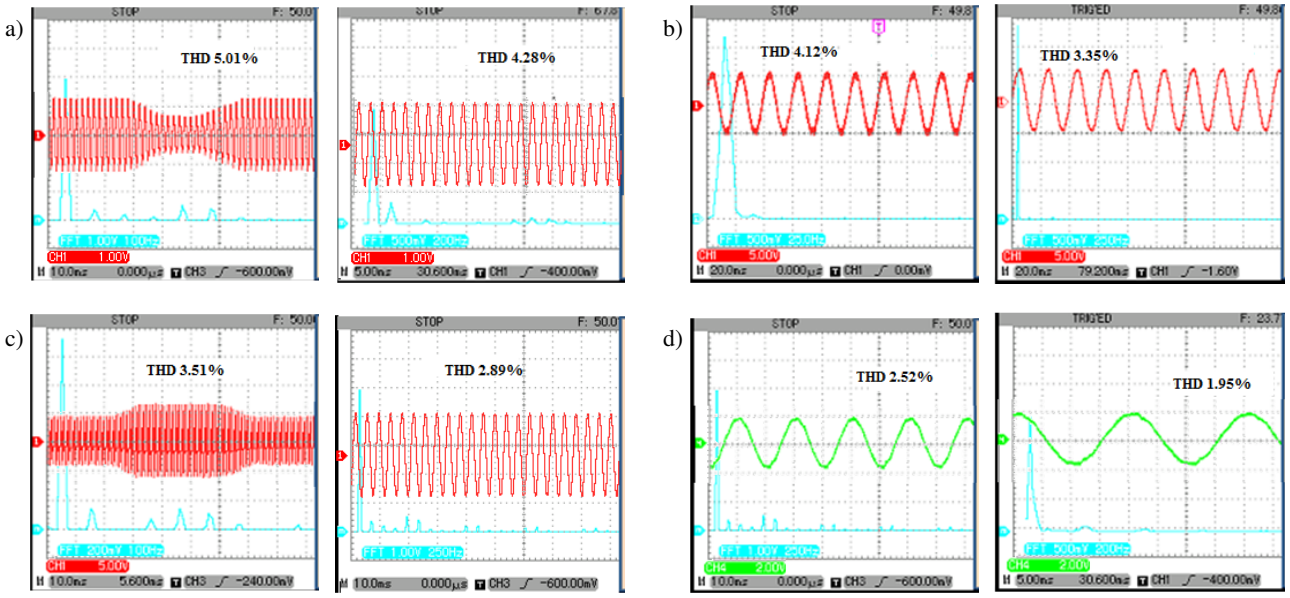

Fig. 11. Sag and Swell load voltage and current: (a) sag source voltage and sag load voltage, (b) sag source current & sag load current, (c) swell source voltage & swell load voltage, (d) swell source current and swell load current

6. CONCLUSIONS

An Intelligent Controller required to manage the UPQC using four single PI and single SCANN has been developed. The simulation model is developed in MATLAB/Simulink platform, and a performance study is done by comparing the conventional PI controller and proposed SCANN controller results. From the results, it is evident that the proposed SCANN controller provides considerable voltage compensation compared to the conventional control technique and helps for power quality improvement. Based on the simulation results obtained from the proposed algorithm, a validated hardware prototype model is developed and tested under different operating conditions. The observed result of the prototype model in terms of THD value and compensation voltage is found close with the simulation results. The proposed SCANN is validated successfully in simulation and the experimental prototype model.

REFERENCES

[1] E. Hossain *et al.*, "Analysis and mitigation of power quality issues in distributed generation systems using custom power devices", *IEEE Access*, vol. 6, pp. 16816–16833, 2018, doi: 10.1109/ACCESS.2018.2814981.

[2] J. Ye, H. Beng Gooi, and F. Wu, "Optimization of the size of UPQC system based on data-driven control design", *IEEE Trans. Smart Grid*, vol. 9, no. 4, pp. 2999–3008, 2018, doi: 10.1109/TSG.2016.2624273.

[3] S. Chandrakala Devi, B. Singh, and S. Devassy, "Modified generalized integrator-based control strategy for solar PV fed UPQC enabling power quality improvement", *IET Gener. Transm. Distrib.*, vol. 14, no. 16, pp. 52–65, 2020, doi: 10.1049/iet-gtd.2019.1939.

[4] S. Silva *et al.*, "Comparative performance analysis involving a three-phase UPQC operating with conventional and dual/inverted power-line conditioning strategies", *IEEE Trans. Power Electron.*, vol 35, no. 11, pp. 11652–11665, 2020, doi: 10. 1109/TPEL.2020.2985322.

[5] S.B. Karanki, M.K. Mishra and B.K. Kumar, "Particle swarm optimization-based feedback controller for unified power-quality conditioner", in *IEEE Trans. Power Del.*, vol. 25, no. 4, pp. 2814-2824, Oct. 2010, doi: 10.1109/TPWRD.2010.2047873.

[6] Y. Bouzelata, E. Kurt, R. Chenni, and N. Altın, "Design and simulation of a unified power quality conditioner fed by solar energy", *Int. J. Hydrogen Energy*, vol. 40, no. 44, pp. 15267–15277, 2015, doi: 10.1016/j.ijhydene.2015.02.077.

[7] N. Kumarasabapathy and P.S. Manoharan, "MATLAB simulation of UPQC for power quality mitigation using an ant colony based fuzzy control technique", *Hindawi Publishing Corporation Scientific World J.*, vol. 2015, pp. 1–10, 2015, doi: 10.1155/2015/304165.

[8] S. Samal and P. Hota, "Power quality improvement by solar photovoltaic / wind energy integrated system using unified power quality conditioner", *Int. J. Power Electron. Drive Syst.*, vol. 8, no. 3, pp. 1416–1426, 2017, doi: 10.11591/ijpeds.v8.i3.pp1416–1426.

[9] M. Gwozdz, R. Wojciechowski, and L. Cieplinski, "Power supply with parallel reactive and distortion power compensation and tunable inductive filter–Part 2", *Bull. Pol. Acad. Sci. Tech. Sci.*, vol. 69, no. 4, pp. 1–9, 2021, doi: 10.24425/bpasts.2021.137938.

[10] S. Vinnakoti and V.R. Kota, "Implementation of artificial neural network-based controller for a five-level converter based UPQC", *Alexandria Eng. J.*, vol. 57, no. 3, pp. 1475–1488, 2018, doi: 10.1016/j.aej.2017.03.027.

[11] A. Dheepanchakkravarthy *et al.*, "Predictive current control of FL-shunt active power filter for dynamic and heterogeneous load compensation", *Electr. Eng.*, vol. 103, no. 4, pp. 2147–2460, 2021, doi: 0.1007/s00202-021-01224-6.

[12] N. Sangeetha, B. Gopinath, S. Muthulakshmi, M. Kalayanasundram, and G. Suriya, "A new approach to single phase AC microgrid system using UPQC device", *Bonfring Int. J. Softw. Eng. Soft Comput.*, vol. 8, no. 2, pp. 26–35, 2018, doi: 10.9756/BIJSESC.8392.

[13] A. Ali *et al*., "Performance evaluation of ZVS/ZCS high efficiency AC/DC converter for high power applications", *Bull. Pol. Acad. Sci. Tech. Sci.*, vol. 68, no. 4, pp. 793–807, 2020, doi: 10.24425/bpasts.2020.134185.

[14] A. Dheepanchakkravarthy, M.R. Jawahar, K. Venkatraman, M.P. Selvan, and S. Moorthi, "Performance evaluation of FPGA based predictive current controller for four-leg DSTATCOM in electric distribution system", *IET Gener. Transm. Distrib.*, vol. 13, no. 19, pp. 4400–4409, 2019, doi: 10.1049/iet-gtd.2019.0073.

[15] C.K. Sundarabalan, Y. Puttagunta, and V. Vignesh, "Fuel cell integrated unified power quality conditioner for voltage and current reparation in four-wire distribution grid", *IET Smart Grid*, vol. 2, no. 1, pp. 60–68, 2019, doi: 10.1049/iet-stg.2018.0148.

[16] M. Ochoa-Gimenez, A. Garcia-Cerrada, J.L. Zamora-Macho, "Comprehensive control for unified power quality conditioners", *J. Mod. Power Syst. Clean Energy*, vol. 5, pp. 609–619, 2017, doi: 10.1007/s40565-017-0303-2.

[17] U.K. Renduchintala and C. Pang, "Neuro-fuzzy based UPQC controller for Power Quality improvement in micro grid system", *IEEE/PES Transm. Distrib. Conf. Exposition*, 2016, pp. 1–5, doi: 10.1109/TDC.2016.7519965.

[18] P. Falkowski, K. Kulikowski, and R. Grodzki, "Predictive and look-up table control methods of a three-level ac-dc converter under distorted grid voltage", *Bull. Pol. Acad. Sci. Tech. Sci.*, vol. 65, no. 5, pp.609–618, 2017, doi: 10.1515bpasts-2017-0066.

[19] B. Rahmani, W. Li, and G. Liu, "A wavelet-based unified power quality conditioner to eliminate wind turbine non-ideality consequences on grid-connected photovoltaic systems", *Energies*, vol. 9, no. 6, pp. 390, 2016, doi: 10.3390/en9060390.

[20] P. Falkowski and A. Godlewska, "Finite control set MPC of LCL-filtered grid-connected power converter operating under grid distortions", *Bull. Pol. Acad. Sci. Tech. Sci.*, vol. 68, no. 5, pp. 1069–1076, 2020, doi: 10.24425/bpasts.2020.134655.